Analysis of OBrO, IO, and OIO absorption signature in UV-visible spectra measured at night and at sunrise by stratospheric balloon-borne instruments

Gwenaël Berthet, Jean-Baptiste Renard, Michel Chartier, Michel Pirre, C Robert

Analysis of OBrO, IO, and OIO absorption signature in UV-visible spectra measured at night and at sunrise by stratospheric balloon-borne instruments

Gwenaël Berthet, Jean-Baptiste Renard, Michel Chartier, Michel Pirre,[1] and Claude Robert
Laboratoire de Physique et Chimie de l'Environnement, CNRS, Orléans, France

Received 28 February 2002; revised 13 September 2002; accepted 31 December 2002; published 8 March 2003.

[1] Absorption bands of OBrO, IO, and OIO in the visible region have been investigated in the data of the AMON ("Absorption par les Minoritaires Ozone et Nox") and SALOMON ("Spectroscopie d'Absorption Lunaire pour l'Observation des Minoritaires Ozone et Nox") balloon-borne spectrometers used to obtain measurements in the nighttime stratosphere, since 1992 and 1998 respectively. The absorption features initially detected in AMON residual spectra and attributed to OBrO are also observable in SALOMON data with better accuracy. New estimates of OBrO cross-section amplitudes taking into account recent laboratory measurements are used for the OBrO retrieval. A consequence is that previously published OBrO concentration and mixing ratio values are revised downwards of around 40%. Further tests are performed to assess the consistency of the OBrO detection. No correlation exists between OBrO and NO_2 vertical profiles which practically rules out the possibility for the structures ascribed to OBrO absorption to be due to remaining NO_2 contributions. It is shown that variability of OBrO quantities at high latitudes obtained from various AMON and SALOMON flights is possibly linked to the chemical processes involving the production of OClO. At midlatitudes, the exceptional and unexpected conditions of the April 28, 1999 SALOMON flight allow us to observe the drop in OBrO concentrations just after sunrise. As expected, if previous studies of stratospheric iodine species are considered, IO and OIO absorption lines are never detected in the residual spectra. The presence of unknown structures in the residual spectra in the IO and OIO absorption regions is obvious and tends to distort the retrievals. The possibility that these remaining features result from a temperature dependence effect or uncertainties of O_3 and/or NO_2 cross-sections is suggested. Thus, more accurate laboratory measurements and sets of cross-sections for low temperature are needed. *INDEX TERMS:* 0340 Atmospheric Composition and Structure: Middle atmosphere—composition and chemistry; 0343 Atmospheric Composition and Structure: Planetary atmospheres (5405, 5407, 5409, 5704, 5705, 5707); 0394 Atmospheric Composition and Structure: Instruments and techniques; 0399 Atmospheric Composition and Structure: General or miscellaneous; *KEYWORDS:* UV-visible spectroscopy, stratosphere, bromine and iodine species

Citation: Berthet, G., J.-B. Renard, M. Chartier, M. Pirre, and C. Robert, Analysis of OBrO, IO, and OIO absorption signature in UV-visible spectra measured at night and at sunrise by stratospheric balloon-borne instruments, *J. Geophys. Res.*, *108*(D5), 4161, doi:10.1029/2002JD002284, 2003.

1. Introduction

[2] In the stratosphere, absorption in the visible region is mainly due to ozone and NO_2. Now, UV-visible spectrometers performing remote measurements using occultation techniques are sensitive enough to detect absorption features with an optical depth of the order of 10^{-4}. This value is about 100 times smaller than typical NO_2 absorption. The instruments can operate from stratospheric balloons, (tropospheric) airplanes, and the ground, using the Sun, Moon or stars as light sources. Three stratospheric species causing only weak absorption spectral signatures in the UV-visible spectral domain are studied: OBrO, IO and OIO.

[3] *Renard et al.* [1998] identified the presence of permanent remaining structures, assigned to the absorption of bromine dioxide (OBrO), in the optical depth spectra of the AMON (French acronym for "Absorption par les Minoritaires Ozone et Nox") balloon-borne instrument performing nighttime measurements. The high values of mixing ratios derived reveal that OBrO could be present at night as the main stratospheric bromine species. Data analysis from the first flight of the SALOMON (French acronym for "Spectroscopie d'Absorption Lunaire pour l'Observation des

[1] Also at Département de Physique, Université d'Orléans, France.

0148-0227/03/2002JD002284

Minoritaires Ozone et Nox'') instrument, the successor of AMON, have also resulted in the detection of the signal ascribed to OBrO [*Renard et al.*, 2000]. New results and further tests are presented in this paper providing more arguments in favor of the presence of OBrO in the nighttime stratosphere. At present, this detection is not confirmed by other instruments, and is in contradiction with modeling results [*Chipperfield et al.*, 1998]. Analysis of nighttime UV-visible measurements performed onboard a Transall airplane have allowed *Erle et al.* [2000] to derive mixing ratios with upper limits at least three times smaller than those given by *Renard et al.* [1998], and to conclude that OBrO does not exist at night. Consequently in order to resolve such opposite conclusions in the OBrO detection, further analysis of the various methods used, and the conditions under which observations are made, is required.

[4] The two iodine species, iodine oxide (IO) and iodine dioxide (OIO), have strongly absorbing vibrational bands in the visible region that can be investigated in the SALOMON data. The role of iodine species, and especially IO, has to be seriously taken into account in the marine boundary layer where they are likely to constitute the main source of the ozone sink [e.g., *Vogt et al.*, 1999]. Thus the interest in measuring iodine species in the stratosphere is obvious, and estimates of stratospheric inorganic iodine mixing ratios have already been conducted by various teams using a variety of instruments [*Berg et al.*, 1980; *Wennberg et al.*, 1997; *Pundt et al.*, 1998; *Wittrock et al.*, 2000]. The understanding of iodine chemistry has recently progressed [*McFiggans et al.*, 2000], even if uncertainties still remain and further laboratory studies are probably needed. Of course, further measurements are necessary before the chemistry of stratospheric iodine is fully understood. To our knowledge, the only published estimates of stratospheric IO upper limits from balloon measurements are those of *Pundt et al.* [1998] derived from averaging measurements obtained at sunset or sunrise, at different locations and periods of the year using a SAOZ spectrometer [*Pommereau and Piquard*, 1994]. They found insignificant IO quantities during daytime when IO is thought to be a major iodine species. At night, it is expected that IO is not present in the stratosphere. Concerning OIO, it seems that there are as yet no published measurements of this species in the stratosphere from UV-visible spectrometers. It is of interest to check the possibility for OIO to be a nighttime reservoir of iodine in the stratosphere. Owing to its high sensitivity, SALOMON data can be used to investigate these two species.

[5] We present below an analysis of SALOMON optical depth spectra in the respective spectral domains of OBrO, IO and OIO. The values of their inferred mixing ratios, or at least their upper limits will be discussed as well as the possible consequences for (nighttime) stratospheric chemistry. SALOMON measurements of OBrO have been conducted at mid and high latitudes during night and, in one case, during sunrise on April 28, 1999 at midlatitudes allowing the study of the possible night-day transition of OBrO. The analysis of the two iodine species is described using the best flight data obtained on December 4, 2000 at high latitudes. The main advantage of this instrument is its self-calibrated method of measurements (the so-called moon occultation method), with a reference spectrum and occultation spectra recorded during the same session of observation. As a result of the mechanical (and thermal) stability of SALOMON, there is no apparent wavelength shift of the position of the spectra on the detector. Thus, the occultation spectra can be divided by the reference spectrum without any correction or assumption concerning the response of the instrument. The sensitivity and accuracy of the instrument is then only limited by the electronic noise of the pixels.

[6] Note that SALOMON, like AMON before it [*Renard et al.*, 1997], can be used for the retrieval of OClO in the near UV domain. Then, the anticorrelation of the vertical profiles of OClO and OBrO inside the polar vortex suggested by AMON measurements can be studied here. For that purpose, new high latitude OBrO measurements by AMON in 1999 are also presented.

2. Observation and Methodology

2.1. Amon and Salomon Instruments

[7] AMON and SALOMON are designed to perform nighttime measurements of stratospheric compounds having spectral features in the visible region: O_3, NO_2, NO_3, OClO and aerosols. To our knowledge, no other instrument conducts measurements in the UV-visible wavelength range from a balloon at night. AMON and SALOMON have operated in the Northern Hemisphere at mid and high latitudes since 1992 and 1998, respectively. They are used routinely, in particular as part of European and satellite validation campaigns. Descriptions of the AMON instrument are reported by *Robert* [1992], *Naudet et al.* [1994], and *Renard et al.* [1996, 2001b]. The performance characteristics of the AMON detector and pointing system have been detailed in the work of *Renard et al.* [1998] on OBrO detection. Similar descriptions of the SALOMON instrument have been provided by *Renard et al.* [2000], and *Berthet et al.* [2001] who describe the improved performances of SALOMON. A summary of these instrumental characteristics is provided below.

[8] The AMON and SALOMON measurement methods are based respectively on the similar principles of stellar and lunar occultation. The stellar occultation method consists of recording the spectrum of a setting star that is modified due to absorption by the atmospheric species along the line of sight. At the balloon float altitude, between 30 and 40 km, a reference spectrum is first recorded when the star is a few degrees above the gondola horizon. Raw occultation spectra are then recorded while the star sets below the gondola horizon, using exposure times between 20 and 50 s. The transmission spectra are obtained by dividing the star occultation spectra with the reference spectrum. They contain the effect of the absorption bands of the atmospheric species but are free of the stellar absorption lines. The optical depth spectra are then calculated by taking the logarithm of the inverse transmission spectra. The measurement is self-calibrating since no assumption concerning the response of the instrument is needed.

[9] AMON is composed of a 20-cm Cassegrain telescope with a 1 m focal length, a grating spectrometer, and a CCD detector of 385 by 578 pixels. The UV-visible spectral range from 350 to 675 nm is covered continuously using five spectral bands (50 or 75 nm wide). Spectra are sampled at 0.18 nm per pixel in the UV band and at 0.14 nm per pixel

in the four visible bands [*Renard et al.*, 1996, 1998]. These resolutions are perfectly tailored for analysis of species absorbing in the near-UV and visible [*Roscoe et al.*, 1996]. Absorption features of different species are analyzed separately in these five bands. The AMON spectrometer is able to detect spectral signatures with a minimum optical depth of 10^{-3}. The observation method gives a vertical resolution between a few hundreds meters in the middle stratosphere and around 1 km in the lower stratosphere. AMON flights have been made under various geophysical conditions from the midlatitude launch base at Aire sur l'Adour (France, 43.7°N, 0.3°W) and from the high-latitude base at Kiruna/Esrange (Sweden, 67.9°N, 22.1°E).

[10] In SALOMON, on-off switching, pointing, data acquisition and telemetry are controlled automatically. SALOMON is composed of a pivot (stabilization unit of the gondola), a moon tracker (rotating turret with a mirror that moves on elevation), and a SAOZ type spectrometer [*Pommereau and Piquard*, 1994] which operates continuously in the near-UV and visible. Spectra are sampled at 0.34 nm per pixel. In order to cover the NO_3 absorption band at 662 nm, the wavelength region of the SAOZ spectrometer has been shifted to 350–700 nm. An optical fiber is used to direct light from the pointing system to the spectrometer providing a very stable system. The spectrometer does not have moving parts and then does not suffer from any kind of mechanical deformations during the moon pointing procedure. Moreover, the instrument is thermally insulated so it is not affected by external temperature variations.

[11] SALOMON is designed to operate between the first and last quarters of the Moon. It takes measurements with high moon-pointing accuracy, both during the ascent of the balloon and at float altitude during a moon-set, but only at float altitude during a moon-rise. The Moon's flux allows this instrument to detect absorption features greater than 10^{-4} which is ten times better than AMON. SALOMON is much less sensitive to pointing problems than AMON and this allows optimized signal-to-noise ratios to be more easily obtained during strong wind conditions. Indeed, as an example, the strong stratospheric wind conditions encountered during the February 22, 2000 flight from Kiruna (up to 270 km/h) did not affect the moon-pointing procedure nor the quality of the spectra. The drawback of SALOMON in comparison with AMON is its vertical resolution, since the apparent size of the Moon (0.5°) does not allow a vertical resolution better than 1–2 km. Flights of SALOMON have been performed also from Aire sur l'Adour and Kiruna launch bases: three during moon-set and two during moon-rise.

2.2. Obtaining Residual Spectra

[12] We describe here briefly the data reduction method that can be found in the papers of *Renard et al.* [1996, 1998, 2000]. The analysis procedure for slant column densities is similar for both instruments.

[13] Cosmic ray traces and dark current are first removed from the spectra. Then wavelength scales are established using, for AMON, the known positions of the H and He lines of the star, and for SALOMON, the main solar absorption lines. AMON is sensitive to chromatic scintillation [e.g., *Renard et al.*, 2001a], unlike SALOMON owing to the Moon's large apparent size. This effect on AMON spectra, that results from the motion of air masses along the line of sight, is reduced using a sliding average procedure over five consecutive spectra. For both the AMON and SALOMON instruments, the noise is reduced by smoothing the spectra using a gaussian filter with various widths chosen according to the species being studied. This filter uses a FFT procedure that cuts the high frequencies due to noise while the value of the flux is preserved over the whole spectral domain. Then, the actual resolution is between 2 and 3 nm.

[14] With AMON spectra, O_3 and NO_2 slant column densities are searched for in the 550–625 nm and 410–470 nm regions, respectively. The one-band spectral window of SALOMON is adequate for the retrieval of a species' absorption features over much larger spectral ranges: roughly from 430 to 680 nm for O_3 and from 400 to 550 nm for NO_2. For both flights presented in this paper, measurements of temperature and pressure profiles were obtained by onboard instruments during the balloon ascent. The Rayleigh scattering contribution is calculated and removed from the spectra using these profiles and the spectral cross-sections given by *Bucholtz* [1995]. Then, O_3 and NO_2 slant column densities are determined by least-squares fits using the University of Bremen high resolution absorption cross-sections measured by S. Voigt, J. Orphal, and J. P. Burrows (unpublished data available from http://www.iup.physik.uni-bremen.de/gruppen/molspec/index.html). These cross-sections are the most recent laboratory data sets and appear to be among the most accurate. Prior to the fit procedure, they are interpolated and smoothed by the gaussian filter to match the resolution resulting from the pixel sampling of the instruments. Very good fits to the spectra observed by SALOMON can be obtained, as shown on Figure 1 with standard deviations between the measurement and the fit of 3×10^{-3} and 1×10^{-3} for O_3 and NO_2 respectively. Slant column density error bars are given by one standard deviation in the least-squares fit. Note that the effect of the contribution of species above the balloon float altitude in the reference spectrum acts as an offset on the slant column profile and is taken into account [*Renard et al.*, 2000, 2001b]. All lines of sight are not used to determine slant column densities since retrieval is performed only when signal-to-noise ratios (computed in our case by the ratio of the fit maximum amplitude to the standard deviation defined above) are greater than 1. Thus, lines of sight close to the tropopause are not considered most of the time.

[15] Since O_3, NO_2, Rayleigh scattering and aerosols constitute the major contributions in the absorption domains of OBrO, IO and OIO, differential residual spectra are finally determined in these spectral regions by removal of O_3 and NO_2 calculated optical depths and by application of a high-pass filter. This filter allows removing the aerosol contribution and low frequency ozone and NO_2 residuals. We note that the subtraction of the species and Rayleigh scattering optical depths over the entire visible region provides optical depth spectra that are attributed to the contribution of stratospheric aerosols [*Berthet et al.*, 2002].

2.3. Observing Conditions

[16] The flights presented in this work took place under various conditions, and a summary is presented on Table 1. The February 12, 1999 measurements by the AMON instrument were conducted inside the polar vortex around 00 UT,

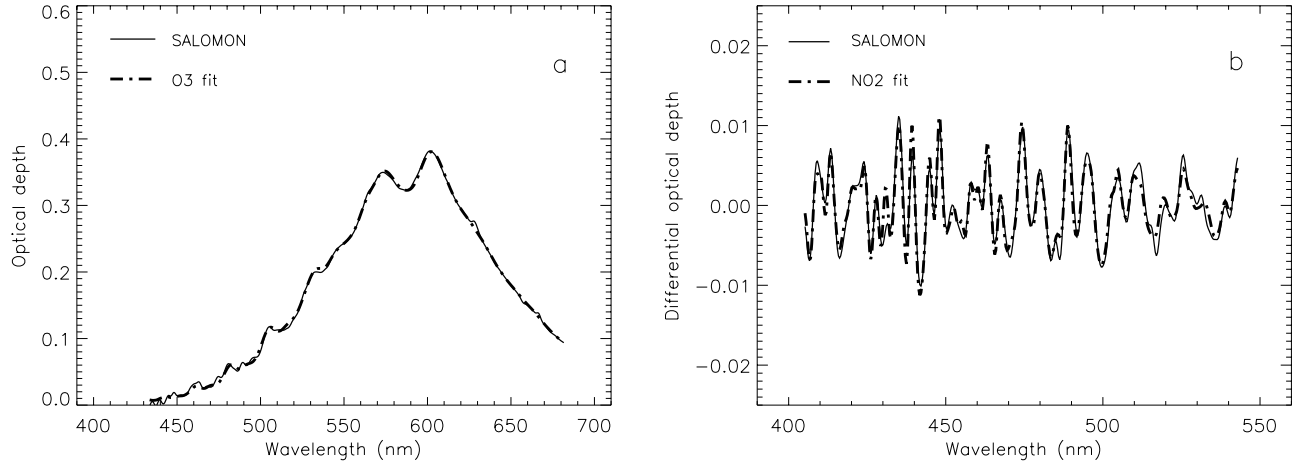

Figure 1. Example of O_3 (a) and NO_2 (b) measured optical depth spectra for the December 4, 2000 SALOMON flight from Kiruna (moon elevation of $-2.5°$). The NO_2 spectrum is obtained after subtraction of the O_3 contribution, and after application of a high-pass filtering procedure which removes low frequencies structures due to aerosols and remaining O_3 contributions.

using the star Alnilam (ε Orionis) whose UV flux is adequate for the OClO retrieval. The April 28, 1999 SALOMON flight took place from Aire sur l'Adour launch base during moon-set. Two days before the full Moon, the flux was high enough for the optimal detection ability of the instrument to be achieved. Measurements were first conducted during balloon ascent around 0230 UT. This flight occurred at the end of the night giving rise to particular measurement conditions that prevented observation of the end of the moon occultation. As a result of the rise of the Sun at 0420 UT, whose flux is at least 100,000 times higher than that of the Moon, the moon-pointing procedure stopped and the SALOMON gondola started to rotate horizontally while the moon-tracker's mirror oscillated vertically. Thereby, since the spectrometer was still running, several spectra containing the spectral signature of the sunlight were recorded with sun elevations between $-6°$ and $-2°$. Only spectra recorded in the field of view of the Sun (or very close) are analyzed since tangent heights and then vertical profiles can be derived. No sun reference spectrum was recorded; nevertheless it was possible to retrieve slant column densities after sunrise using the moon reference spectrum recorded at float since no wavelength shift between the moon reference spectrum and the sunlight spectra has been detected. The difference between the global shape of the spectra and the moon reference spectrum gives rise to low frequencies that are eliminated by the high-pass filtering procedure.

[17] Two high-latitude SALOMON flights are complementary for the study presented in this paper. The January 23, 2000 SALOMON flight was conducted around 1630 UT from Kiruna inside the polar vortex. Because of the trajectory of the balloon, the flight was stopped before the end of moon occultation, and only profiles between 12 and 18 km were obtained. The February 22, 2000 SALOMON flight was performed around 1900 UT from Kiruna on the edge of the polar vortex, 3 days after full Moon allowing high signal-to-noise ratios to be obtained.

[18] SALOMON was also launched on December 4, 2000 from Kiruna, and the measurements were conducted around 2130 UT. This flight occurred during the setting of the first moon quarter inside the polar vortex. The float altitude was the highest of the SALOMON flights (34 km), which allowed the benefit firstly of a high-quality reference spectrum free at best from the contributions of species present above the gondola, and secondly of long integration paths leading to strong absorption during occultation. Several improvements had been made since the previous flights: first, since the accuracy of the pointing system was improved for this flight, the pointing system reached its optimal performance even during these low flux moon phase conditions never used before (15% of the full Moon). Secondly, as far as the quality of the spectra is concerned, the transmission of the optical system was increased resulting in optimized signal-to-noise ratios. Thirdly, the use of a new optical fiber allowed the usable spectral range to be

Table 1. Conditions of Measurements

Date	Time, TU	Location	Experiment	Altitude, km	Species Analyzed
1997-02-26	22:00	High latitudes	AMON	17–31	O_3, NO_2, OClO, OBrO
1999-02-12	00:00	High latitudes	AMON	17–29	O_3, NO_2, OClO, OBrO
1999-04-28	02:30	Midlatitudes	SALOMON		Night:
				22–31	Ascent: O_3, NO_2
				29–31	Occultation: O_3, NO_2, OBrO, IO, OIO
	04:30				Sunrise:
				10–26	O_3, NO_2, OBrO, IO, OIO
2000-01-23	16:30	High latitudes	SALOMON	14–18	O_3, NO_2, OClO, OBrO
2000-02-22	19:00	High latitudes	SALOMON	17–29	O_3, NO_2, OClO, OBrO
2000-12-04	21:30	High latitudes	SALOMON	16–32	O_3, NO_2, OClO, OBrO, IO, OIO

Table 2. Summary of Mixing Ratios[a]

	26 Feb. 1997	12 Feb. 1999	28 April 1999 Night	28 April 1999 Sunrise	23 Jan. 2000	22 Feb. 2000	4 Dec. 2000
OClO	10–20	30–70			10–40	10–45	0
OBrO	0–11	0–15	11	0	0	0	0–12
IO				1.1 ± 1.2			1.0 ± 1.2
OIO				1.5 ± 1.5			0.2 ± 1.2

[a]Units are in pptv. The variation ranges are given for OClO and OBrO. Upper limits are given for IO and OIO at night.

extended from 390 nm to 340 nm, allowing in particular better retrieval of the OClO contribution. Owing to all the improved performances described here, in this paper we focus particularly on the SALOMON data from this flight.

[19] It is very important to note that for all the SALOMON flights, no significant wavelength shift of the Fraunhofer lines and no instrumental resolution changes between the first and the last recorded spectra have been detected. For instance, the deviation of the position of the lines is less than 0.05 pixels (i.e. 0.017 nm) for the December 4, 2000 flight spectra, for the two-hour session of observation. Such ideal conditions allow the direct division of the occultation spectra by the reference spectrum, pixel by pixel without either wavelength shift adjustment or squeeze, so preventing the appearance of artificial spectral features. Any adjustments to the wavelength scale are then unnecessary for a minimization of the spectra residuals whatever the spectral range. The fact that the data reduction of SALOMON measurements requires few corrections and no a priori hypothesis justifies the following analysis of the residual spectra.

3. Analysis of Residual Spectra: Retrieval of the Halogen Species

[20] A summary of the mixing ratios of the halogen species derived from the analysis of measurements is given in Table 2.

3.1. OBrO Detection

[21] The permanent absorption features remaining in the 475–550 nm region of the residuals of AMON spectra from the February 26, 1997 flight have been attributed to OBrO absorption as described in details by *Renard et al.* [1998]. This detection is confirmed in the high latitude flight data obtained by SALOMON on December 4, 2000. These spectral lines were also observed at midlatitudes by AMON, and by SALOMON on the flights of October 31, 1998 [*Renard et al.*, 2000] and April 28, 1999. All the AMON results presented in this work have been updated since the previous publications. The sets of cross-sections (O_3, NO_2, OBrO, OClO) used are the same as those used for SALOMON data reduction. Same smoothing and filtering parameters and same spectral range are now used for the OBrO retrieval from SALOMON and AMON measurements, and a more regular vertical sampling is used for inversion of AMON slant columns.

3.1.1. OBrO in the Polar Vortex

3.1.1.1. December 4, 2000 Salomon Flight

[22] The December 2000 flight provides the first detection of OBrO in the polar vortex by SALOMON with a higher accuracy than AMON. After the removal of ozone and NO_2 contributions, very good fits of the residual optical depth spectra using the OBrO cross-sections measured at University of Bremen by O. C. Fleischmann, M. Hartmann, and J. P. Burrows (private communication) are obtained over the spectral range restricted to 470–530 nm for an optimal quality of the fits (Figure 2). These cross-sections, assumed to have a maximum of about 1.6×10^{-17} cm^2 similar to that of OClO in the work of *Renard et al.* [1998], have been normalized in order to adjust their absolute values to the recent results of *Knight et al.* [2000]. Since the measurements of *Knight et al.* [2000] have been performed at 298 K, our normalization factor takes into account an estimation of their OBrO cross-section amplitudes for stratospheric temperature conditions, drawing on the temperature variations of OClO cross-section amplitudes (the OClO cross-sections used here were recently measured by *Kromminga et al.* [1999] and are available on the University of Bremen internet site). These new estimated amplitudes of OBrO absorption lines have a maximum of about 2.3×10^{-17} cm^2 and decrease the OBrO mixing ratios previously published by a factor 1.4. The profile of the OBrO mixing ratios versus pressure is plotted on Figure 3d.

[23] Tests have been conducted by *Renard et al.* [1998] to assess possible causes that could generate the structures attributed to the OBrO signature. These investigations have suggested that these spectral features probably do not originate from contamination by other species. For instance, the authors raised the possibility that the remaining spectral

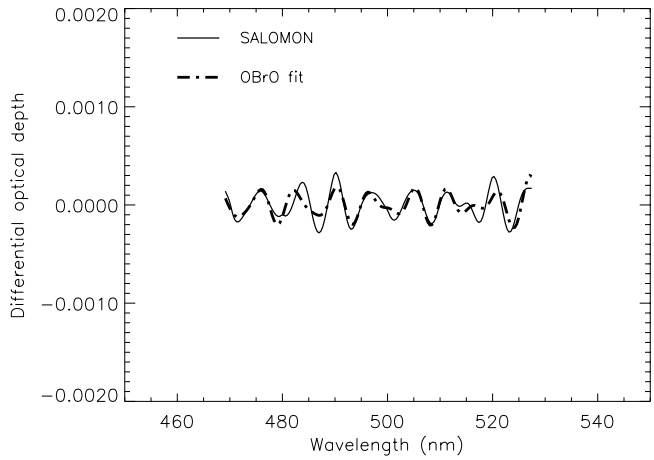

Figure 2. Optical depth spectrum for the December 4, 2000 SALOMON flight (moon elevation of −2.5°) and the least-squares fit with OBrO cross-sections measured at University of Bremen. The signal-to-noise ratio is greater than 6.

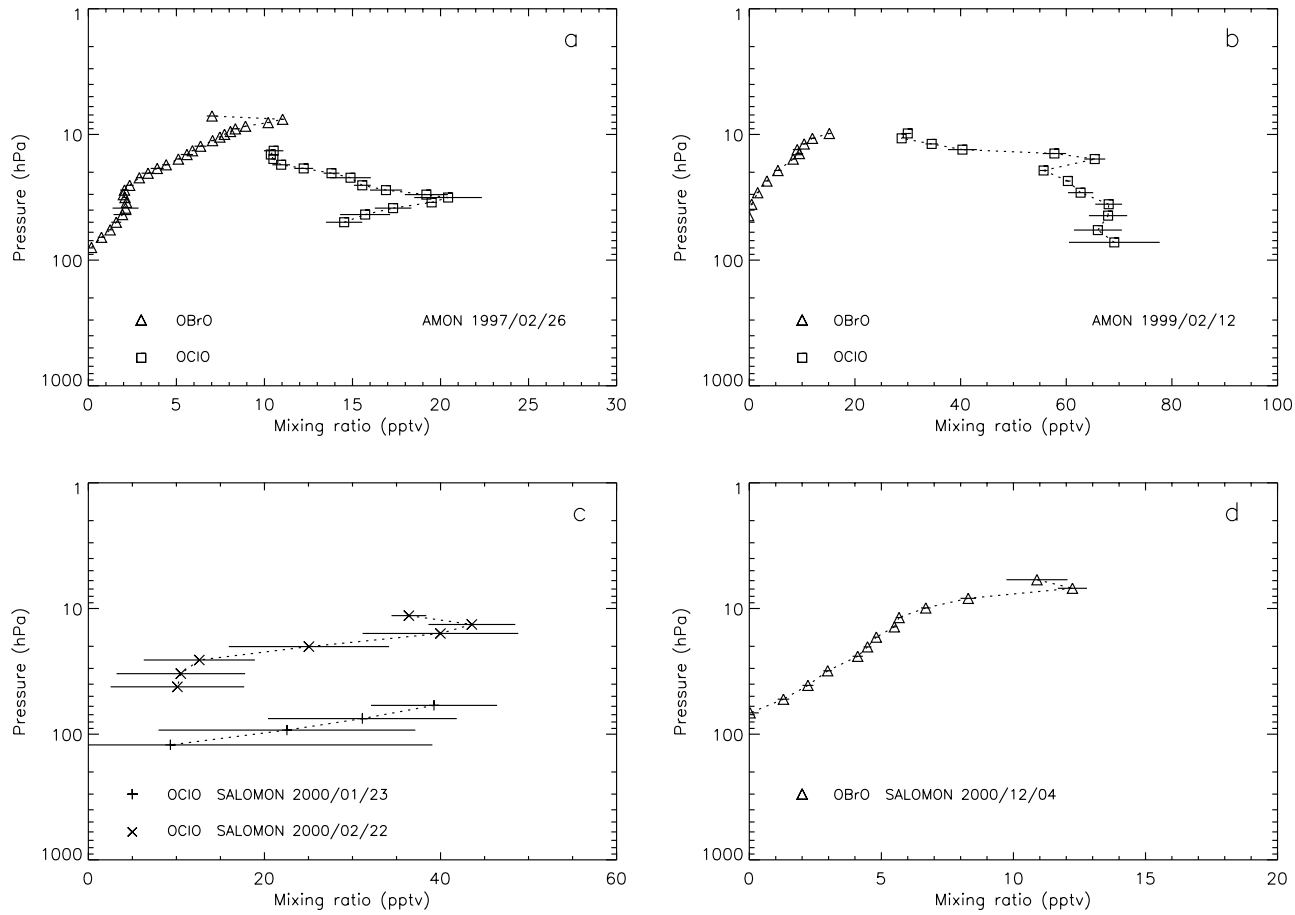

Figure 3. OBrO and OClO mixing ratio vertical profiles from various AMON and SALOMON high-latitude flights. SALOMON and AMON data reductions are performed using the same sets of OBrO and OClO cross-sections measured at University of Bremen as described in the text. (a) comparison of OBrO and OClO profiles obtained from the February 26, 1997 AMON flight conducted inside the polar vortex. (b) same as (a) but for the February 12, 1999 AMON flight also conducted inside the polar vortex. (c) OClO profiles from the January 23, 2000 and February 22, 2000 SALOMON flights conducted respectively inside the polar vortex and on the edge of the vortex. Spectral signatures attributed to OBrO have not been detected from these two flights data. (d) OBrO profile from the December 4, 2000 SALOMON flight conducted inside the early polar vortex. No presence of OClO has been detected.

features could result from possible uncertainties of the NO_2 cross-sections (e.g. amplitude variations, undetected structures, wavelength shift). This seems unlikely if firstly we consider that the NO_2 cross-sections measured by various teams are in agreement and, if secondly we refer to the tests performed by Renard et al. on the weak effect of NO_2 cross-sections uncertainties on the residual structures. After examination of the NO_2 and OBrO concentration vertical profiles obtained after inversion (Figure 4), one can note the absence of a correlation between the two profiles. This can be considered as another indication that the spectral features attributed to OBrO are not the result of any kind of NO_2 residual contamination.

[24] A further test consists of subtracting the optical depth spectra retrieved using OBrO cross-sections from the measured optical depth residuals in the 470–530 nm spectral domain. Figure 5 presents for each moon elevation the optical depth standard deviation values of the spectral residuals compared to that of the residuals after removal of the signal attributed to OBrO. It appears that the correction of the raw residuals using OBrO computed optical depths leads systematically to a reduction of the residuals, from 30 to 50% for the best lines of sight, that is, between -2.0 and $-3.5°$. The values obtained are then very close to the detection limit of the instrument.

[25] As said in the [*Renard et al.*, 1998] paper with AMON measurements, the slant column retrieval is not very sensitive to the smoothing procedure and to the high-pass filter. A new example, using this time SALOMON measurements, is presented on Figure 6. The slant column profile presented on the left is retrieved after using best-optimized parameters, smoothing over 9 pixels and removing the eight first low frequencies, and the profile presented on the right is retrieved after using smoothing over 6 pixels and removing five frequencies. Taking into account the errors bars, which are obviously larger for the less smoothed profile retrieval, the profiles are in excellent agreement. Based on this test, one can conclude that the slant column profiles do not result from specific filtering and smoothing values.

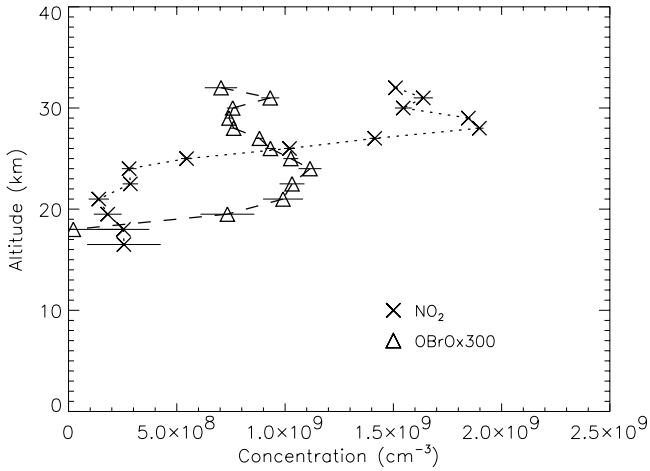

Figure 4. Comparison of vertical profiles of OBrO and NO_2 concentrations from the December 4, 2000 flight. The OBrO profile is increased by a factor 300 for the comparison. No obvious correlation is observable between the two profiles.

[26] The last possibility of misidentification could come from uncertainties on NO_2 cross-sections and their temperature dependence. Figure 7 shows the variation of the OBrO slant column profile when the NO_2 contribution is determined and removed using the NO_2 cross-sections at different temperatures in respect with the 223 K cross-sections. Even with temperatures unrealistic for the stratosphere, the difference is often smaller than 10 percent, thanks to the large spectral domain used which contains a large number of noncorrelated OBrO and NO_2 lines.

[27] Thus it is clear that these structures are neither due to noise nor to well-identified bias on the retrieval. They are consistently present in the spectra of a given flight and clearly identified in the data of two different instruments, with better accuracy for SALOMON than for AMON. This is the clue that these absorption features initially detected in AMON data were not the result of an instrumental bias since the two instruments do not consist of the same optical system and detectors.

3.1.1.2. Simultaneous Measurements of OBrO and OClO

[28] In previous studies [e.g., *Renard et al.*, 1997], the OClO contribution was retrieved from AMON spectra using the laboratory data of *Wahner et al.* [1987]. The OClO cross-sections used at present are those measured by *Kromminga et al.* [1999].

[29] Drawing on the comparison of OBrO and OClO mixing ratio profiles from AMON measurements in the polar vortex, *Renard et al.* [1998] have suggested that the observed amounts of OClO could prevent the production of a large quantity of OBrO. The possible anti-correlation between OClO and OBrO is visible in the profiles from the February 12, 1999 high latitude flight of AMON (Figure 3b) which confirms the tendency already observed in the February 26, 1997 AMON profiles (Figure 3a).

[30] Other cases can be analyzed from the three high latitude SALOMON flights conducted during various geophysical conditions. The signature attributed to OBrO is not detectable for the flights of January 23, 2000 and February 22, 2000, where large amounts of OClO were observed (Figure 3c). The case of the December 4, 2000 flight conducted inside the early vortex seems to be noteworthy. No OClO was detected since large amounts of NO_2 were present during this flight which was performed before any chlorine activation occurred.

3.1.2. Diurnal Variation of OBrO at Midlatitude: April 28, 1999 SALOMON Flight

[31] The time and duration of the April 28, 1999 SALOMON flight have allowed the study of the diurnal variation of the measured stratospheric chemical species. Such a study has already been performed for NO_2 by *Payan et al.* [1999] using the measurements of two different balloon-borne instruments, AMON and LPMA.

[32] The signature ascribed to OBrO absorption cannot be detected in the ascent measurements since the total air mass was too low (in that case, the signal to noise ratio does not allow to detect absorption features smaller than 10^{-3}). However, despite shorter lines of sight than during the December 2000 SALOMON flight, the possible OBrO signal has been detected in the moon occultation measurements from the April 1999 flight. Even though the amplitude of the absorption lines is weak since the measurement stopped just after the beginning of the occultation procedure (resulting in vertical profiles only from 29 to 31 km), the residual optical depths in the 470–530 nm spectral range have been successfully fitted by OBrO cross-sections (Figure 8) giving signal-to-noise ratios up to 4. Mixing ratios of 11 pptv are obtained in this small altitude range.

[33] Let us now focus on the measurements performed after sunrise. Because of the free motion of the gondola and of the mirror, various "light sources" have contributed to the recorded spectra. The contribution of blue sky light is not negligible and has to be corrected for in these spectra. For that purpose, sunlight spectra are normalized so that the ozone slant column density profile gives the best fit to a model ozone slant column profile typical for midlatitudes.

[34] Before searching for the possible absorption of OBrO at daytime, the diurnal evolution of NO_2 has to be

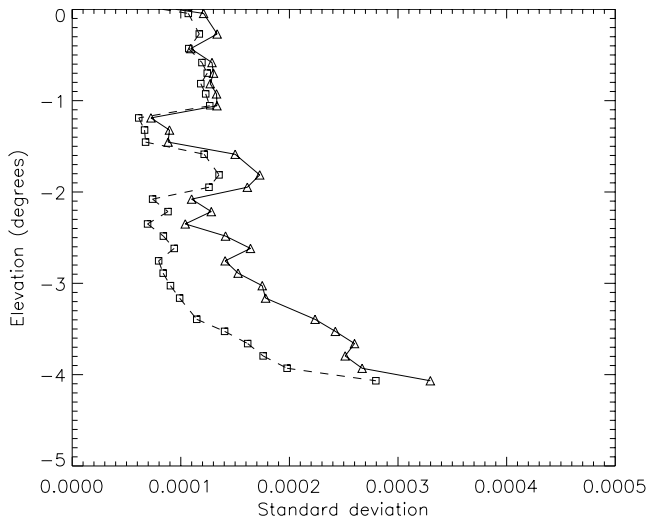

Figure 5. Optical depth standard deviations of the residuals for each moon elevation for the December 4, 2000 flight (triangles). The residuals removed from the signal ascribed to OBrO gives reduced standard deviations (squares).

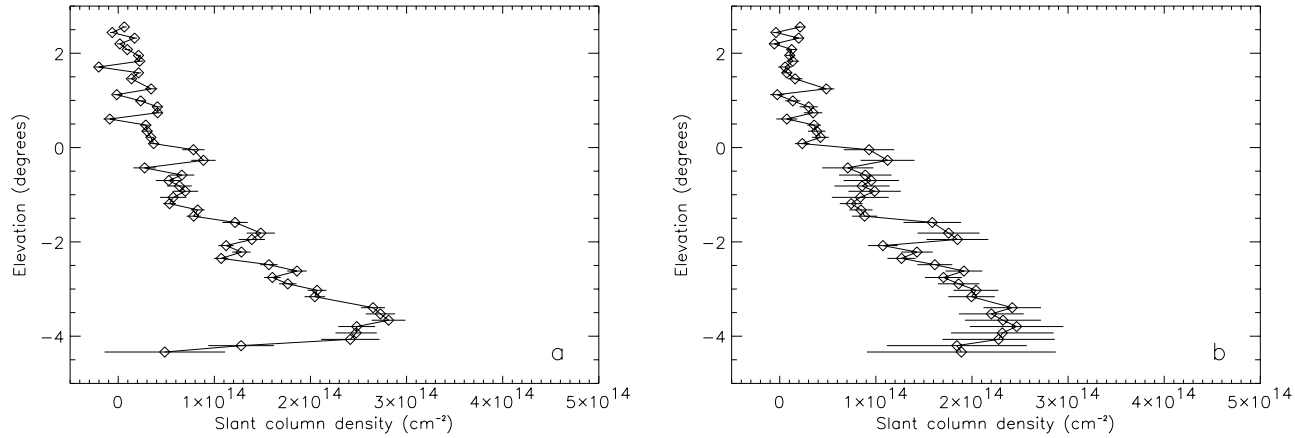

Figure 6. Slant column profile for the December 4, 2000 flight. Left: smoothing over 9 pixels and removing of the eight first frequencies. Right: smoothing over 6 pixels and removing of the five first frequencies. Taking into account the errors bars, the two profiles are in excellent agreement.

studied. As for ozone, these concentration profiles (ascent, moon occultation, sun occultation) corresponding to different times between 0230 UT and 0500 UT have been retrieved (Figure 9). The low number of usable sunlight spectra leads to a wide and variable vertical resolution of 2 to 5 kilometers. Nevertheless, vertical profiles have been obtained between 11 and 30 km for daytime since the complete occultation of the Sun has been observed. One can see in Figure 9 the reduction of NO_2 quantities above 20 km at daytime as expected. Outputs from a photochemical box model version of the lagrangian model MIPLASMO [*Rivière et al.*, 2000] have been used in order to reproduce the diurnal variation of NO_2 for comparison with the measurements. For the midlatitude conditions of this flight, the evolution of the NO_2 concentration from nighttime to sunrise is strongly dependent on ozone concentration and temperature [e.g., *Payan et al.*, 1999]. The model is initialized using the NO_2 concentration retrieved from the measurements performed during the balloon ascent. We have assumed that for each altitude the measurements have been conducted within the same air parcel. This is a reasonable assumption considering the small distance between the nighttime and the sunrise measurements (that is, only 250 to 350 km), the short time delay and the stability of the ozone concentration profiles during the night-day transition. This modeling study reveals the coherence between the measured moonset and sunrise profiles and gives confidence in the analysis of the sunlight spectra for the retrieval. Another remark can be made here. The highly photodissociative species NO_3, always observed at night by AMON and SALOMON [*Renard et al.*, 2001b], has not been detected after sunrise which reinforces the confidence in the data reduction method.

[35] The same spectral range and the same smoothing and filtering data reduction parameters as for moon occultation spectra have been used for the analysis of the sunlight spectra. Just after sunrise, that is, a few minutes after the moon occultation measurements, the signal attributed to

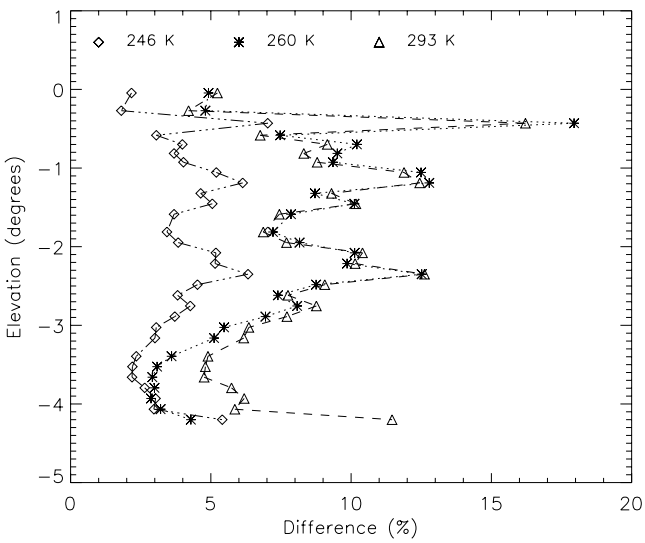

Figure 7. Variation of the OBrO slant column profile when using NO_2 cross-sections at different temperatures in respect to the 223 K cross-section. Even with temperatures unrealistic for the stratosphere, the difference is often smaller than 10 percent.

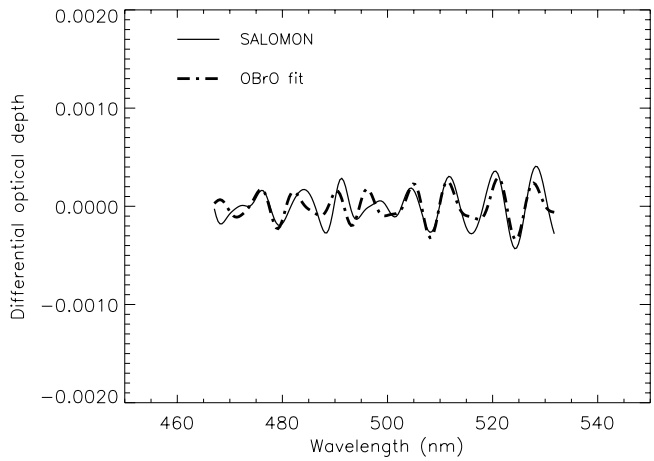

Figure 8. Optical depth spectrum for the April 28, 1999 SALOMON flight (moon elevation of −1.6°) and the least-squares fit with the OBrO cross-section. The signal-to-noise ratio is greater than 4.

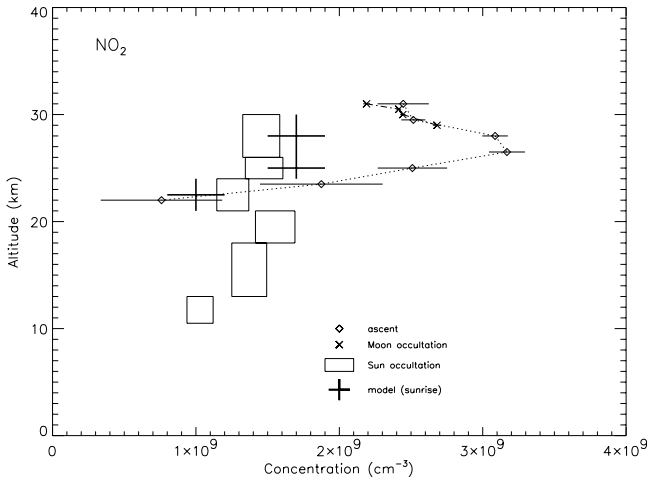

Figure 9. NO_2 concentration profiles from ascent, moon occultation and sun occultation measurements of the April 28, 1999 SALOMON flight. NO_2 concentrations after sunrise are compared with model results. Model calculations uncertainties are provided by uncertainties in concentrations measured at ascent used to initialize the model.

OBrO seems to disappear (Figure 10) whatever the line of sight. The spectrum presented in Figure 10 has been recorded for an elevation of $-5.2°$ corresponding to a line of sight nearly tangent to the tropopause (usable here since the signal recorded by the spectrometer is higher than during a moon occultation), which gives an optical path length more favorable for species absorption than the case of the December 2000 flight presented in Figure 2. Unfitted residual structures with peak-to-peak optical depths up to 5×10^{-4} remain (the amplitude of this residual is higher than on other figures since the line of sight is very low). The weak fit in Figure 10 by the OBrO cross-sections can be considered as a statistical detection allowing the provision of upper limits for OBrO quantities at daytime. It should be noted that in the adequate observing conditions of the Figure 10 spectrum, the presence of OBrO would have led to peak-to-peak optical depths of 10^{-3} assuming the midlatitude OBrO quantities measured on October 16, 1993 by AMON. Then, for the profile between 10 and 26 km, a value of 0.2 pptv is observed which is largely below the values measured during moon occultation.

[36] Therefore it is obvious that these SALOMON observations have revealed a fast drop in OBrO amounts after sunrise. Such a result is in agreement with the theoretical prediction that this molecule is highly photodissociative.

[37] The NO_2 night-day transition presented in Figure 9 reveals a decrease roughly by a factor 2, above 25 km after sunrise whereas OBrO values fall almost to zero. Consequently, we have here once again an indication that the OBrO and NO_2 retrievals are independent.

3.2. Retrieval of Iodine Monoxide (IO) and Iodine Dioxide (OIO)

3.2.1. Previous Studies of IO and OIO

[38] *Solomon et al.* [1994] suggested that the coupling of stratospheric chlorine and bromine chemistry with iodine compounds such as IO could play an important role in the lower stratospheric ozone depletion processes via rapid catalytic cycles. However, taking into account more recent measurements of kinetic parameters and of stratospheric total iodine abundance lower than the 1 pptv assumed by *Solomon et al.* [1994], this role of iodine compounds at mid and high latitudes has been significantly reduced [*Wennberg et al.*, 1997; *Pundt et al.*, 1998], unless, as suggested by these authors, iodine chemistry is different from that assumed at present.

[39] The first published estimation of the total iodine mixing ratio in the lower stratosphere (<0.3 pptv for midlatitudes) was reported by *Berg et al.* [1980] from measurements aboard aircraft and balloon sampling platforms. Up to now, measurements of IO and OIO were mostly performed by ground-based instruments during daytime. The estimation of the contribution of stratospheric IO (with expected amounts below 1 pptv) from ground-based instrument data is difficult due to the stronger contribution in general of tropospheric IO (that can reach about 6 pptv in the marine boundary layer according to the results of *Alicke et al.* [1999]), and thus requires the use of photochemical model outputs. For instance, *Wittrock et al.* [2000] have estimated stratospheric IO mixing ratios in the range 0.65–0.80 (±0.2) pptv above Spitsbergen whereas the findings of *Frieß et al.* [2001] have revealed no evidence for stratospheric presence of IO in their measurements from Antarctica. The ground-based measurements of *Wennberg et al.* [1997] from Kitt Peak observatory in Arizona have given total iodine mixing ratios of 0.2 (+0.3 −0.2) pptv. It is consistent with the upper limits derived from the balloon-borne measurements at mid and high latitude of *Pundt et al.* [1998] in the morning and evening (0.3 pptv at 20 km and 0.15 pptv at 15 km). Nevertheless, a variability is observed in the above results obtained from different instruments and for different times and locations. This suggests that stratospheric (and tropospheric) iodine chemistry (especially its seasonal and geographical variability) is not completely understood and requires further investigation. It is, however, well accepted that the total inorganic iodine at daytime is dominated by the active forms of iodine species, I and IO (IO_x) that are

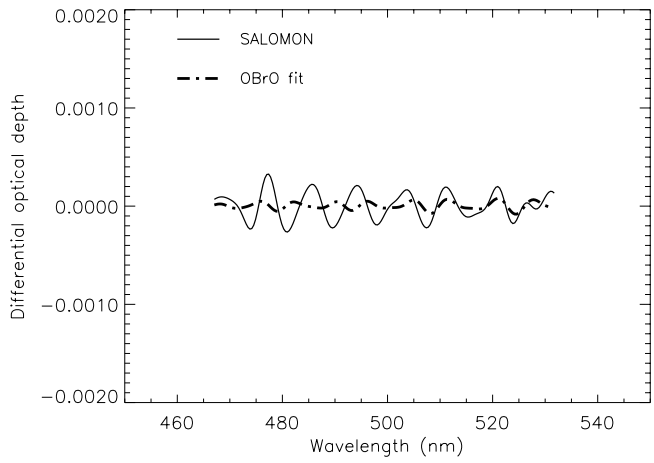

Figure 10. Optical depth spectrum for the April 28, 1999 SALOMON flight obtained after sunrise (sun elevation of $-5.2°$) and the least-squares fit with the OBrO cross-section. No evidence of OBrO absorption is observed.

produced by photolysis of precursor species [e.g., *Alicke et al.*, 1999]. IO_x recombines at night into its reservoir species according to various modeling studies for troposphere or stratosphere [*Solomon et al.*, 1994; *Wennberg et al.*, 1997; *Vogt et al.*, 1999; *McFiggans et al.*, 2000]. In that case, the stratospheric IO signature should not be present in SALOMON data.

[40] Concerning OIO, its formation is thought to originate from the self-reaction of IO, with OIO as the major product [*McFiggans et al.*, 2000], and from the reaction of IO with BrO [*Cox et al.*, 1999]. Indeed, the first laboratory observations of OIO by *Himmelmann et al.* [1996] as well as the more recent measurements of *Cox et al.* [1999] have revealed that OIO is chemically coupled to IO. Moreover, surprisingly, it appears that OIO could be highly stable towards photolysis [*Cox et al.*, 1999]. According to modeling studies [e.g., *Cox et al.*, 1999; *McFiggans et al.*, 2000], under the favorable conditions of the marine boundary layer, OIO could become an important gas phase reservoir of iodine and could limit the ozone destruction from the iodine species channel. Unfortunately, observations of OIO in the atmosphere are very rare and are limited to the marine boundary layer [*Allan et al.*, 2001]. The results of *Allan et al.* [2001] reveal a diurnal variability of OIO amounts, with a maximum of 2–3 ppt after sunset, but most of the time values are below 0.5 ppt even at night. With such a low value in the favorable conditions of formation in the marine boundary layer, OIO is expected to be undetected in the stratosphere and to be below the detection limit of SALOMON.

3.2.2. Analysis of the SALOMON Residual Spectra in the IO Spectral Domain

[41] Figure 11 shows the same residual spectrum from the December 4, 2000 flight as Figure 2 but in the 400–460 nm spectral region with the fit of the IO cross-sections from University of Bremen (S. Himmelmann, personal communication). Note that the OBrO contribution has been removed in the spectral domain used for the IO retrieval. In the case of Figure 11, the signal-to-noise ratio is below 1 and there is absolutely no evidence of an IO signature. The weak detection in Figure 11 is caused by residual features tending to distort the fits with, in particular, unidentified structures clearly present in the spectrum around 431 nm. Various smoothing and filtering parameters were used to test the sensitivity of the resulting slant column profile. It appears that the profile is sensitive to the smoothing and filtering procedures which seems to indicate that the residual spectra in the range of 400–460 nm are mainly contaminated by noise and/or residual structures from other species. Therefore, as a criterion, the parameters have been chosen so that the value of the residual is minimized (standard deviation of 2×10^{-4} for the case of Figure 11). We can remark that the inversion of the slant column profile yields a large mixing ratio range with 1.0 ± 1.2 pptv between 22 and 33 km. Because of the bias in the fits described above, it is not possible here to estimate a more accurate IO mixing ratio upper limit, especially if this value is extremely close to 0 pptv which seems to be the case at night according to models predictions. We are clearly below the detection limit of a species by the instrument.

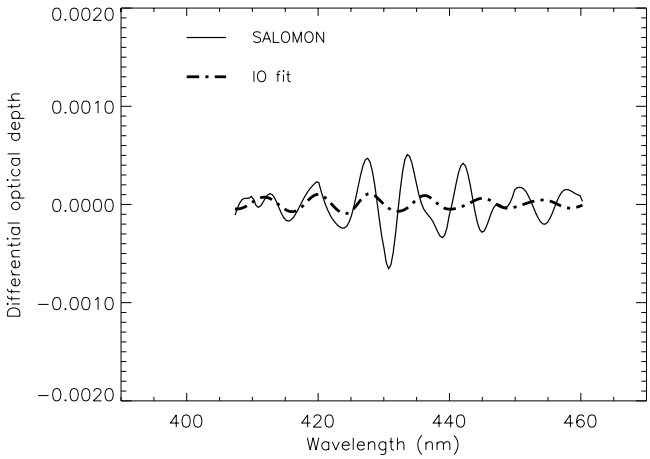

Figure 11. Optical depth spectrum for the December 4, 2000 SALOMON flight (moon elevation of −2.5°) and the least-squares fit with IO cross-sections measured at University of Bremen. Smoothing and filtering parameters are similar to those used for OBrO retrieval. The fit is distorted by a residual structure around 431 nm but no evidence of IO absorption is found.

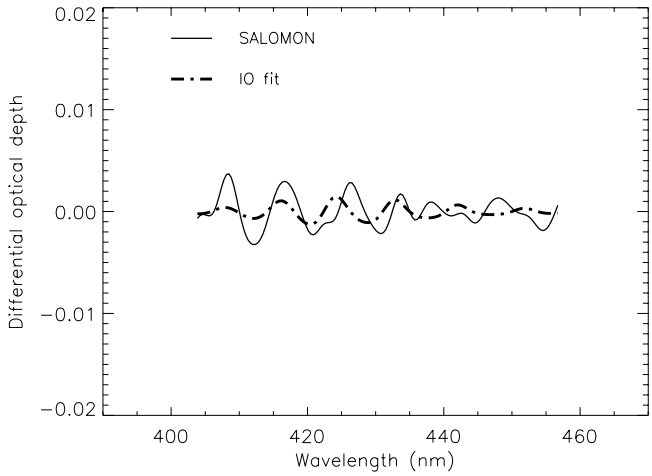

Figure 12. Optical depth spectrum for the April 28, 1999 SALOMON flight obtained after sunrise (sun elevation of −5.2°) and the least-squares fit with the IO cross-section. The fit is also distorted by residual structures.

[42] Daytime IO mixing ratios are expected to be a few tenths of pptv at best. The signal-to-noise ratios of the April 28, 1999 flight spectra recorded after sunrise are too low to allow us to investigate accurately a possible stratospheric IO diurnal variation. Indeed, sunrise spectra are distorted by residual structures and once again, no evidence of an IO signal is found (Figure 12). The distorted fits result in large mixing ratios values of 1.1 ± 1.2 pptv between 10 and 26 km.

3.2.3. Analysis of the SALOMON Residual Spectra in the OIO Spectral Domain

[43] The December 4, 2000 residual spectrum is represented in Figure 13 over the 520–600 nm spectral domain. The OIO cross-sections used, which have a shape close to that of the OBrO cross-sections, have also been measured at University of Bremen [*Himmelmann et al.*, 1996]. The standard deviation of the residual features is very low (1.4

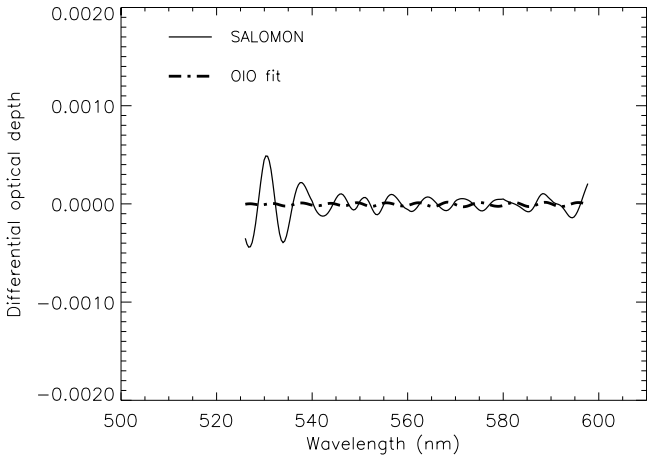

Figure 13. Optical depth spectrum for the December 4, 2000 SALOMON flight (moon elevation of −2.5°) and the least-squares fit with OIO cross-sections measured at University of Bremen. Smoothing and filtering parameters are similar to those used for OBrO retrieval. OIO is not detected.

$\times 10^{-4}$) and clearly, there is no sign of any OIO absorption. The very weak fit observed (with peak-to-peak amplitude of 5×10^{-5} in Figure 13) results in mixing ratios of 0.2 ± 1.2 pptv between 22 and 33 km.

[44] In the sunrise spectra of the April 28, 1999 flight, large residual structures (with standard deviations of 3×10^{-3}) distorting the fits are once again present, preventing estimations of a consistent upper limit of OIO after sunrise. The distortion of the fits leads to mixing ratio values no more precise than 1.5 ± 1.5 pptv.

4. Discussion and Conclusions

[45] The permanent residual spectral features attributed to OBrO in the work of *Renard et al.* [1998] are clearly detected in SALOMON residual spectra and are present at the same wavelength locations. Judging by the quality of the fits, they are characterized by a greater accuracy than the AMON results on account of SALOMON's better sensitivity. These stable structures give rise to very similar mixing ratio values in the polar vortex being determined from the December 4, 2000 SALOMON and the February 26, 1997 AMON flights, taking into account new estimations of OBrO absorption line amplitudes [*Knight et al.*, 2000]. Nevertheless, as derived from AMON measurements by *Renard et al.* [1998] and apparently confirmed by results using SALOMON data, a variability of OBrO amounts, as well as OClO amounts, seems to be observed during flights by both instruments in the polar vortex. The comparison of the various evolutions of OBrO and OClO mixing ratio profiles could lead us to speculate that this variability is governed by the chemical processes involving the formation of OClO. These processes appear to be incompletely understood like the interaction between halogen and nitrogen species [*Rivière et al.*, 2003]. However, our hypothesis could improve our understanding of the chemical mechanisms resulting in the possible generation of OBrO in the stratosphere. New observations conducted during various geophysical conditions, time and locations are necessary to test our hypothesis.

[46] The possible evolution of OBrO between the end of the night and sunrise was established here at midlatitude. The signal attributed to OBrO disappears rapidly after sunrise which is theoretically expected for this photodissociative species. This result constitutes a further step towards consistency in the possible detection of OBrO.

[47] At present no other instrument has confirmed the possible presence of OBrO in the stratosphere. Nighttime upper limits of stratospheric OBrO have been derived by *Erle et al.* [2000] from direct moon-light spectra recorded from the troposphere onboard a Transall aircraft during various geophysical conditions, times and locations. Their mixing ratio values (< 6.4 ppt) are at least three times lower than values derived from AMON measurements. They have however concluded that no OBrO signature is detected by their DOAS instrument which has sufficiently low threshold to detect low absorption features such as those attributed to OBrO. The estimation of the optical depth upper limit of OBrO possibly present in the DOAS spectra residual is calculated by use of a statistical formula [*Stutz and Platt*, 1996]. Then, upper limit of mixing ratio values are inferred using the assumption of a Gaussian shaped OBrO concentration profile peaking at 28 km. Actually, Erle et al.'s. measurements are not directly comparable to our results since observing conditions and data reduction method were different.

[48] As stated above, the SALOMON detector does not suffer from temperature variation effects. Two strong Na solar lines are present around 589 nm and no evidence of them remains in the 520–600 nm residual spectra (Figure 13). Furthermore, there is no trace of a residual of the main Fraunhofer lines on the optical depth spectra. Thus, the residual structures around 431 nm that distort nighttime IO retrieval cannot be the result of a remaining Fraunhofer line. The shape and amplitude of these structures seem to vary from flight to flight, with notably much lower amplitudes for midlatitude data. Besides, the temperatures encountered inside the vortex during the December 2000 flight were the coldest among all the SALOMON flights. Since cross-sections corresponding to the lowest temperatures that can be encountered inside the polar vortex (typically below 200 K) are not available at present, we speculate that the residual structures around 431 nm are the result of the temperature dependence of ozone or NO_2 cross-sections (such an effect would act on the intensity of the NO_2 absorption lines rather than on the position of these lines [*Harder et al.*, 1997]). Concerning the removal of the ozone contribution, this effect is likely to entail the presence of remaining low frequencies [*Renard et al.*, 1998] especially in the spectral region where the ozone cross-sections are weaker, that is, roughly below 500 nm. In any case, the identification of the 431 nm line requires further measurements and investigation and is beyond the scope of this paper.

[49] The problem of temperature dependence of the O_3 and NO_2 cross-sections on remote-sensing measurements has been pointed out by recent studies with the help of scientists involved in laboratory and atmospheric measurements (Johannes Orphal, report for European Space Agency, 2001). In particular, there are some small discrepancies for the amplitude and/or the position of the lines at some wavelengths between the various sets of data. This could

partly explain the presence of unknown permanent structures in the absorption region of OBrO, IO, and OIO (Figures 10, 11, 12, and 13). An incomplete removal of the ozone and NO_2 contributions is also likely to occur on account of the inadequate absolute accuracy of their cross-sections. Indeed, the data from the various flights reveal that SALOMON measurements are more accurate than the cross-sections measured in laboratories, owing to the detector sensitivity and the long integration path of the measurement. Therefore, some of the permanent residual structures could be the result of cross-sections uncertainties. This justifies the following recommendation from the recent investigations described above: the necessity of determining cross-sections with an improved absolute accuracy in the UV-visible region, that is, better than 2%, appears to be urgent. Although the OBrO mixing ratio profiles are not correlated with O_3 and NO_2 profiles, such an improvement would give increased confidence in the possible presence of OBrO in the nighttime stratosphere.

[50] As expected, the absorption lines of the two iodine species, IO and OIO, were not detected by SALOMON. The same result was observed for all flights. Thus, it can be noticed that the data reduction procedure does not lead systematically to a positive detection of a species. Even though more accurate upper limits for the IO mixing ratio cannot be derived from SALOMON nighttime measurements since the fits tend to be distorted by residual structures, we conclude that the results of *Wennberg et al.* [1997] and *Pundt et al.* [1998] are confirmed. As mentioned in passing in the work of *Wennberg et al.* [1997], three possible conclusions can be inferred from the nondetection of OIO by SALOMON: (1), the transport of inorganic and organic iodine to the mid and high latitude stratosphere via tropical convective systems (initially suggested by *Solomon et al.* [1994]) is too weak; (2), OIO is an insignificant nighttime stratospheric iodine reservoir in comparison with other potential reservoirs such as HOI and $IONO_2$; and (3), iodine species are removed by means of heterogeneous chemistry on stratospheric aerosols. The study of the second hypothesis requires measurements in the stratosphere of the possible iodine key species described by *McFiggans et al.* [2000], which would help to gain a better understanding of the homogeneous chemistry processes involving iodine species. Laboratory measurements are at present necessary to check the last hypothesis concerning in particular a possible uptake of OIO on sulfate aerosols. Indeed, iodine chemistry cannot be suitably understood without a detailed study of the heterogeneous chemistry processes.

[51] In summary, using a new estimation for the absolute values of the cross-sections, OBrO mixing ratios around 15 pptv could be present in the middle stratosphere at mid-latitude, while lower mixing ratios are detected at high latitude when tens of pptv are observed for OClO. During daytime, no OBrO is detected, as expected since this species is highly photodissociative. Both IO and OIO are not detected in the middle and lower stratosphere with an upper limit of 1 pptv. Contrary to the OBrO detection, this result is in agreement with modeling results. It confirms that the iodine species do not play a significant role in the stratospheric ozone chemistry.

[52] Nighttime remote sensing measurements of stratospheric species will be performed in the visible domain by onboard satellite instruments GOMOS (using the stellar occultation method like AMON), SCIAMACHY (owing to its lunar occultation mode) and SAGE III (owing also to its lunar occultation mode). However, if we consider the sensitivity threshold of these instruments, small absorption features such as those attributed to OBrO will be very difficult to detect as well as upper limits of IO and OIO amounts. Nevertheless, averaging a large number of spectra recorded in similar geophysical conditions could allow deriving an estimation of such contributions.

[53] Actually, nighttime balloon-borne measurements by other instruments of the halogen species studied in this paper are necessary so that they can be compared directly to AMON and SALOMON results. Whether OBrO detection in the nighttime stratosphere is confirmed or not, the present knowledge of bromine chemistry is incomplete since measurements of stratospheric bromine key species such as $BrONO_2$ and BrCl have never been performed. New instruments have to be developed for that purpose.

[54] **Acknowledgments.** The authors would like to thank all the members of the CNES launching team at Aire sur l'Adour and Kiruna, and the Geneva Observatory team who operates the AMON gondola. This work is supported by the French Program of Atmospheric Chemistry (PNCA) and by various European Commission contracts.

References

Alicke, B., K. Hebestreit, J. Stutz, and U. Platt, Iodine oxide in the marine boundary layer, *Nature*, *397*, 572–573, 1999.

Allan, B. J., J. M. C. Plane, and G. McFiggans, Observations of OIO in the remote marine boundary layer, *Geophys. Res. Lett.*, *28*, 1945–1948, 2001.

Berg, W. W., P. J. Crutzen, F. E. Grahek, S. N. Gitlin, and W. A. Sedlacek, First measurements of total chlorine and bromine in the lower stratosphere, *Geophys. Res. Lett.*, *7*, 937–940, 1980.

Berthet, G., J.-B. Renard, M. Chartier, C. Robert, M. Pirre, J.-P. Pommereau, F. Goutail, and P. François, *Proceedings of the 15th ESA Symposium on European Rocket and Balloon Programmes and Related Research*, *Eur. Space Agency Spec. Publ.*, *ESA-SP-471*, 623–627, 2001.

Berthet, G., J.-B. Renard, C. Brogniez, C. Robert, M. Chartier, and M. Pirre, Optical and physical properties of stratospheric aerosols from balloon measurements in the visible and near-infrared domains, 1, Analysis of aerosol extinction spectra from the AMON and SALOMON balloon-borne spectrometers, *Appl. Opt.*, *41*, 7522–7539, 2002.

Bucholtz, A., Rayleigh-scattering calculations for the terrestrial atmosphere, *Appl. Opt.*, *34*, 1227–1230, 1995.

Chipperfield, M. P., T. Glassup, I. Pundt, and O. V. Rattigan, Model calculations of stratospheric OBrO indicating very small abundances, *Geophys. Res. Lett.*, *25*, 3575–3578, 1998.

Cox, R. A., W. J. Bloss, R. L. Jones, and D. M. Rowley, OIO and the atmospheric cycle of iodine, *Geophys. Res. Lett.*, *26*, 1857–1860, 1999.

Erle, F., U. Platt, and K. Pfeilsticker, Measurements of OBrO upper limit in the nighttime stratosphere, *Geophys. Res. Lett.*, *27*, 2217–2220, 2000.

Frieß, U., T. Wagner, I. Pundt, K. Pfeilsticker, and U. Platt, Spectroscopic measurements of tropospheric iodine oxide at Neumayer Station, Antarctica, *Geophys. Res. Lett.*, *28*, 1941–1944, 2001.

Harder, J. W., J. W. Brault, P. V. Johnston, and G. H. Mount, Temperature dependent NO_2 cross-sections at high spectral resolution, *J. Geophys. Res.*, *102*, 3861–3879, 1997.

Himmelmann, S., J. Orphal, H. Bevensmann, A. Richter, A. Ladstätter-Weissenmayer, and J. P. Burrows, First observation of the OIO molecule by time-resolved flash photolysis absorption spectroscopy, *Chem. Phys. Lett.*, *251*, 330–334, 1996.

Knight, G., A. R. Ravishankara, and J. B. Burkholder, Laboratory studies of OBrO, *J. Phys. Chem.*, *104*, 11,121–11,125, 2000.

Kromminga, H., S. Voigt, J. Orphal, and J. P. Burrows, UV-Visible FT spectra of OClO at atmospheric temperatures, in *Proceedings of the* 1st *European Symposium on Atmospheric Measurements From Space*, Eur. Space Agency, Paris, France, 1999.

McFiggans, G., J. M. C. Plane, B. J. Allan, and L. C. Carpenter, A modeling study of iodine chemistry in the marine boundary layer, *J. Geophys. Res.*, *105*, 14,371–14,385, 2000.

Naudet, J.-P., C. Robert, and D. Huguenin, Balloon measurements of stratospheric trace species using a multichanel UV-visible spectrometer, in

Proceedings of the 14th ESA Symposium on European Rocket and Balloon Programs and Related Research, *Eur. Space Agency Spec. Publ.*, *ESA-SP-355*, 165–168, 1994.

Payan, S., C. Camy-Peyret, P. Jeseck, T. Hawat, M. Pirre, J.-B. Renard, C. Robert, F. Lefèvre, H. Kanzawa, and Y. Sasano, Diurnal and nocturnal distribution of stratospheric NO_2 from solar and stellar occultation measurements in the Arctic vortex: comparison with models and ILAS satellite measurements, *J. Geophys. Res.*, *104*, 21,585–21,593, 1999.

Pommereau, J.-P., and J. Piquard, Ozone and nitrogen dioxide vertical distributions by UV-visible solar occultation from balloons, *Geophys. Res. Lett.*, *21*, 1227–1230, 1994.

Pundt, I., J.-P. Pommereau, C. Phillips, and E. Lateltin, Upper limit of iodine oxide in the lower stratosphere, *J. Atmos. Chem.*, *30*, 173–185, 1998.

Renard, J.-B., M. Pirre, C. Robert, G. Moreau, D. Huguenin, and J. M. Russell III, Nocturnal vertical distribution of stratospheric O_3, NO_2, and NO_3 from balloon measurements, *J. Geophys. Res.*, *101*, 28,793–28,804, 1996.

Renard, J.-B., F. Lefèvre, M. Pirre, C. Robert, and D. Huguenin, Vertical profile of night-time stratospheric OClO, *J. Atmos. Chem.*, *26*, 65–76, 1997.

Renard, J.-B., M. Pirre, C. Robert, and D. Huguenin, The possible detection of OBrO in the stratosphere, *J. Geophys. Res.*, *103*, 25,383–25,395, 1998.

Renard, J.-B., M. Chartier, C. Robert, G. Chalumeau, G. Berthet, M. Pirre, J.-P. Pommerreau, and F. Goutail, SALOMON: A new, light balloon-borne UV-visible spectrometer for nighttime observations of stratospheric trace-gas species, *Appl. Opt.*, *39*(3), 386–392, 2000.

Renard, J.-B., F. Dalaudier, A. Hauchecorne, C. Robert, T. Lemaire, M. Pirre, and J.-L. Bertaux, Measurement of stratospheric chromatic scintillation by balloon-borne spectrometer AMON-RA, *Appl. Opt.*, *40*(24), 4254–4260, 2001a.

Renard, J.-B., F. G. Taupin, E. D. Rivière, M. Pirre, N. Huret, G. Berthet, C. Robert, and M. Chartier, Measurements and simulation of stratospheric NO_3 at mid and high latitudes in the Northern Hemisphere, *J. Geophys. Res.*, *106*, 32,387–32,400, 2001b.

Rivière, E. D., et al., Role of lee waves in the formation of solid polar stratospheric clouds: Case studies from February 1997, *J. Geophys. Res*, *105*, 6845–6853, 2000.

Rivière, E. D., M. Pirre, G. Berthet, J.-B. Renard, F. G. Taupin, N. Huret, M. Chartier, and B. Knudsen, On the interaction between nitrogen and halogen species in the arctic polar vortex during THESEO and THESEO 2000, *J. Geophys. Res.*, *108*(D5), 8311, doi:10.1029/2002JD002087, 2003.

Robert, C., Réalisation d'un spectromètre stellaire multicanal embarquable sous ballon stratosphérique, Ph.D. thesis, Univ. of Orléans, Orléans, France, 1992.

Roscoe, H. K., D. J. Fish, and R. L. Jones, Interpolation errors in UV-visible spectrometry for stratospheric sensing: Implications for sensitivity, spectral resolution, and spectral range, *Appl. Opt.*, *35*, 427–432, 1996.

Solomon, S., R. R. Garcia, and A. R. Ravishankara, On the role of iodine in ozone depletion, *J. Geophys. Res.*, *99*, 20,491–20,499, 1994.

Stutz, J., and U. Platt, Numerical analysis and error estimation of differential optical absorption spectroscopy measurements least-squares methods, *Appl. Opt.*, *35*, 6041–6053, 1996.

Vogt, R., R. Sander, R. Von Glasow, and P. J. Crutzen, Iodine chemistry and its role in halogen activation and ozone loss in the marine boundary layer: A model study, *J. Atmos. Chem.*, *30*, 375–395, 1999.

Wahner, A., G. Tyndall, and A. Ravishankara, Absorption cross-sections for OClO as a function of temperature in the wavelength range from 240–490 nm, *J. Phys. Chem.*, *91*, 2734, 1987.

Wennberg, P. O., J. W. Brault, T. F. Hanisco, R. J. Salawitch, and G. H. Mount, The atmospheric column abundance of IO: Implications for stratospheric ozone, *J. Geophys. Res.*, *102*, 8887–8898, 1997.

Wittrock, F., R. Müller, A. Richter, H. Bovensmann, and J. P. Burrows, Measurements of iodine monoxide (IO) above Spitsbergen, *Geophys. Res. Lett.*, *27*, 1471–1474, 2000.

G. Berthet, M. Chartier, M. Pirre, J.-B. Renard, and C. Robert, LPCE-CNRS, 3A Avenue de la Recherche Scientifique, 45071 Orléans cedex 2, France. (jbrenard@cnrs-orleans.fr)